Cone–Photoreceptor Density in Adolescents With Type 1 Diabetes

Wylie Tan,[1,2] Tom Wright,[1] Durgaa Rajendran,[1] Yaiza Garcia-Sanchez,[1] Laura Finkelberg,[1] Marsha Kisilak,[3] Melanie Campbell,[3] and Carol A. Westall[1,4]

[1]Department of Ophthalmology and Vision Sciences, The Hospital For Sick Children, Toronto, Canada
[2]School of Optometry and Vision Science, University of Waterloo, Waterloo, Canada
[3]Department of Physics and Astronomy, University of Waterloo, Waterloo, Canada
[4]Department of Ophthalmology and Vision Sciences, University of Toronto, Toronto, Canada

Correspondence: Carol A. Westall, Department of Ophthalmology and Vision Sciences, The Hospital for Sick Children, 555 University Avenue, Toronto, Canada M5G 1X8; carol.westall@sickkids.ca.

WT and TW contributed equally to the work presented here and should therefore be regarded as equivalent authors.

Submitted: March 6, 2015
Accepted: August 25, 2015

Citation: Tan W, Wright T, Rajendran D, et al. Cone–photoreceptor density in adolescents with type 1 diabetes. *Invest Ophthalmol Vis Sci*. 2015;56:6339–6343. DOI:10.1167/iovs.15-16817

Purpose. Changes to retinal structure and function occur in individuals with diabetes before the onset of diabetic retinopathy. It is still unclear if these changes initially affect vascular or neural retina, or if particular retinal areas are more susceptible than others. This paper examines the distribution of cone photoreceptor density in the retina of adolescents with type 1 diabetes.

Methods. This cross-sectional prospective study includes 29 adolescents and young adults with type 1 diabetes and no diabetic retinopathy and 44 control participants recruited at the Hospital for Sick Children. Adaptive-optics enhanced retinal imaging of the cone photoreceptor mosaic was performed in four quadrants at an eccentricity of ~7° from the fovea. After image registration and averaging, cone photoreceptors were counted and photoreceptor density was calculated. Analysis of variance with repeated measures was used to assess the differences in photoreceptor density between groups.

Results. Cone density was similar in both control participants and participants with diabetes. There was a small effect of retinal hemisphere; participants with diabetes did not show the expected radial asymmetry observed in control participants.

Conclusions. Cone density in the parafoveal retina is not reduced in adolescents with type 1 diabetes.

Keywords: type 1 diabetes, retina, adaptive optics, adolescent

The neural retina of people with diabetes has been shown to have atypical function and structure. A number of electrophysiological studies have reported deficits of retinal functions in multiple layers of the retina.[1–4] Structural damage to the neural retina has been reported in animals and people with diabetes. A recent study demonstrated a reduction in photoreceptor density close to the fovea of adults with type 1 diabetes (T1D).[5] Animal models have shown cell death and thinning of specific retinal layers shortly after experimental induction of diabetes. Most notable, photoreceptor apoptosis occurred as early as 4 weeks after the onset of diabetes in streptozotocin-induced diabetic rats; by 24 weeks, there was a dramatic reduction of the outer nuclear layer.[6] Neural apoptotic cell death was also observed in postmortem humans with diabetes and no clinically apparent diabetic retinopathy (DR).[7]

Diabetic retinopathy is a progressive disease. Classification of disease severity is primarily based on examination of the fundus either directly or with fundus photography. In addition, disruption of the retinal vasculature is studied using fluorescein angiography. Adaptive optics (AO) retinal imaging is a noninvasive tool that enables high resolution imaging of the retina, in vivo. Adaptive optics–enhanced imaging has demonstrated subclinical changes to the retinal vasculature in people with diabetes, including increased capillary tortuosity, potential drop-out of arterial-venule capillaries,[8] increases in the wall to lumen ratio of retinal arterioles, and increased parafoveal capillary diameter in individuals with diabetes.[9]

Previous work in our lab with the multifocal electroretinogram has shown global retinal dysfunction but no regional susceptibility.[10,11] The purpose of the current study is to examine the effect of T1D on the structural integrity of the outer retina and to determine if there are regional susceptibilities for photoreceptor deficit. Using AO-enhanced scanning laser ophthalmoscopy (AOSLO) we compare cone photoreceptor density between adolescents and young adults with T1D and control participants.

Methods

Subjects

Adolescents and young adults with T1D and no DR were recruited from The Hospital for Sick Children. Inclusion criteria were duration of T1D of ≥5 years and age 10 to 25 years. Participants with any signs of DR were excluded based on 7-field, 30° stereoscopic fundus photographs graded by a retinal specialist according to the modified Airlie House classification system.[12] Typically-developing, age-similar participants without diabetes, recruited from the community, acted as control participants. All participants with other eye diseases, hemoglobinopathy, high refractive error (worse than ±5 diopters [D]),

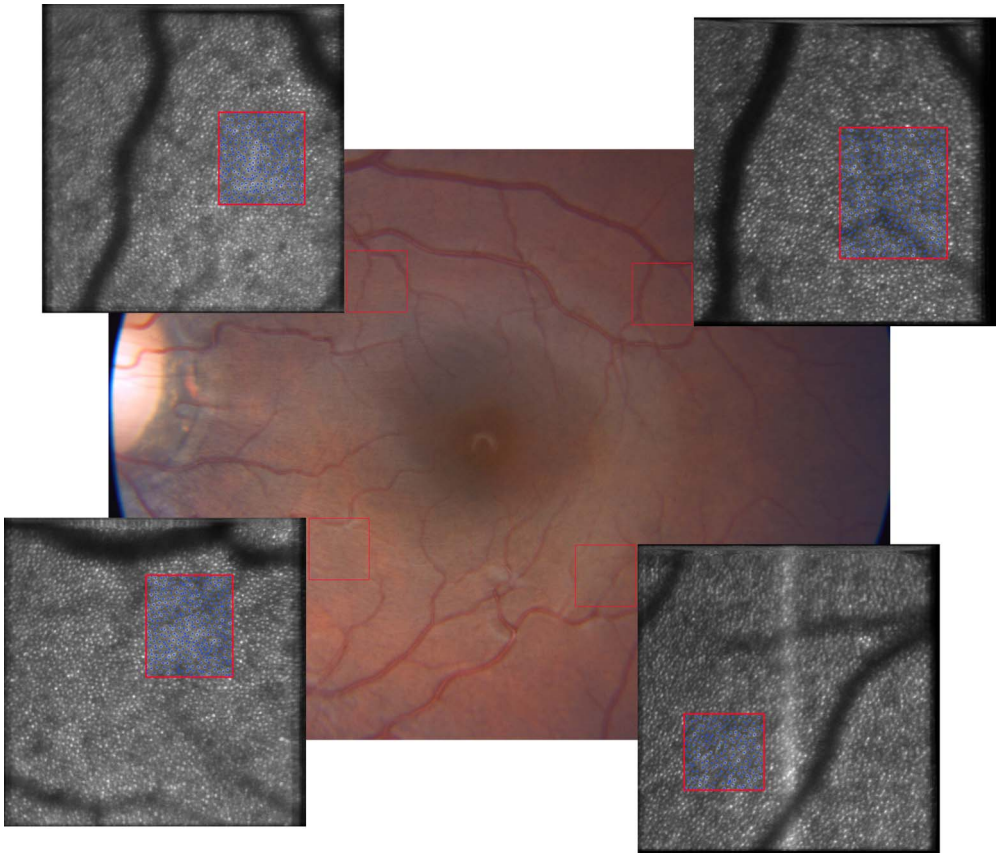

FIGURE 1. Imaging protocol superimposed on a fundus photograph of the right eye of a participant with T1D and no DR. *Red squares* show the regions targeted for AO imaging; *squares* on the AO-enhanced images show the regions selected for cone counting. *Blue dots* indicate cones identified by the automated algorithm.

poor visual acuity (worse than 0.3 logMAR), neurologic disorders, and those on medications affecting retinal function were excluded. Informed consent was obtained from all participants. All procedures were conducted in compliance with the tenets of the Declaration of Helsinki and were approved by the Research Ethics Board at The Hospital for Sick Children.

Data Acquisition

All participants were tested at The Hospital for Sick Children. One eye was selected randomly for testing from each participant and the untested eye was occluded. All participants were assessed for visual acuity (Early Treatment of Diabetic Retinopathy Study vision chart, logMAR), contrast sensitivity (Pelli-Robson), and color vision (Hardy-Rand-Rittler pseudoisochromatic plates and the Mollon-Reffin Minimalist Test). The tested eye was anesthetized with a topical corneal anesthetic (0.5% proparacaine) and dilated pharmacologically (1% tropicamide and 2.5% phenylephrine). Refractive error was measured post dilation for the majority of participants. In participants where refraction was not performed, uncorrected visual acuity was tested to rule out large refractive errors. Axial length from the front corneal vertex to the anterior retina was measured using an I^3 system—ABD ultrasound (Innovative Imaging, Inc., Sacramento, CA, USA). Glycated hemoglobin (HbA1c) values were obtained from a review of hospital charts, only the value closest in time; within 6 months of the AO imaging session was considered. Valid HbA1c values (within 6 months of testing) were not available for 15 participants with T1D.

AO Imaging

Retinal imaging was performed using a multimodal AO retinal imaging system (Physical Sciences, Inc., Andover, MA, USA).[13] Retinal structure was assessed using the scanning laser ophthalmoscope (SLO) channel of the system. The SLO operated at a wavelength centered at 760 nm. Scanning in a raster pattern, the SLO operated at a frame rate of 24 Hz, creating 1024 × 1000 pixel images. The images were taken while focusing on the photoreceptor layer. The AOSLO is capable of resolving retinal structures ~3 μm apart. The imaging protocol is outlined in the fundus photograph in Figure 1. The SLO videos, 1.8° × 1.8° in size, were taken at each retinal quadrant, these areas were centered approximately 5° horizontal × 5° vertical from the fovea.

Optimal participant alignment was achieved by centering the pupil on the wavefront sensor and keeping the AO image bright while locating the field in the line scanning ophthalmoscope (LSO) channel of the AO system. The wide-field LSO beam operated at a wavelength of 915 nm, covering a field diameter of 33° on the retina.

Participant Alignment

Participants were seated in front of the imaging system with their head stabilized between temple and chin rests. The three-axis stage permitted the participant to be moved in the lateral (*x-y* axes) and axial (*z*-axis) directions. Continuous alignment adjustments were made by the operator throughout testing. Participants were asked to fixate on a target and to ignore the scanning laser.

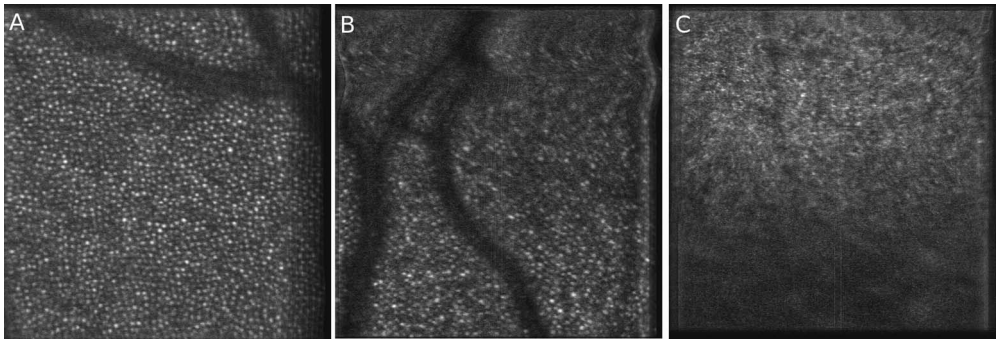

FIGURE 2. Representative SLO images. (**A**) Photoreceptor mosaic visible over entire image. (**B**) Photoreceptor image visible in part of image. (**C**) Photoreceptor mosaic not visible; this image was excluded from further analysis.

Image Analysis

Each SLO video consisted of 30 to 100 frames. Videos were postprocessed to generate the final cone density value, using custom software, as follows: abnormally dim frames, normally caused by participant blinks during recording, were automatically removed. A frame from each video, with no eye movement artifacts, was manually selected. A strip registration algorithm[14] was used to register the remaining frames to this key-frame. After frame registration, three to eight frames with the greatest correlation to the key frame were averaged together to form a final image for cone counting. Cone counting was performed only on images where the cone photoreceptor mosaic was visible in at least part of the image (Fig. 2). Cone counting was performed using custom software based on the Mahotas image processing library.[15] A region, no smaller than $0.2^\circ \times 0.2^\circ$ in size,[16] of each registered image with high quality visualization of the cone photoreceptor mosaic was sampled. Care was taken to avoid large blood vessels when selecting the sampled areas. The selected sample was processed with a two-dimensional Gaussian filter and an intensity threshold calculated using the Otsu method.[17] The number of regions exceeding the threshold was counted and divided by the size of the sampled region (measured in degrees of visual field). This value is reported as the angular cone density. The cone counting algorithm was validated against counts obtained using the graph theory and dynamic programming algorithm proposed by Chiu et al.[18] with data from Garrioch et al.[19] (mean difference = −5%, 95% limits of agreement = −12% to 3%). Cone density calculated as cones per millimeters squared were also calculated based on individual participant axial length measurements. In cases where axial length was not measured, axial length was estimated using a linear model relating refractive error to axial length based on participant data where both measures were available.

TABLE. Demographic Data for All Participants

	T1D Participants, $n = 29$	Control Participants, $n = 44$
Sex, male/female	18/11	12/32
Age at testing, y	19.06 ± 3.0	18.51 ± 3.36
Age at diagnosis, y	8.44 ± 4.7	N/A
Duration of T1D, y	10.69 ± 3.9	N/A
HbA_{1c}, % (n)	8.5 ± 1.3 (14)	N/A
Visual acuity, logMAR (n)	−0.04 ± 0.14 (26)	−0.05 ± 0.11 (42)
Refractive error, D (n)	−1.32 ± 1.2 (15)	−0.81 ± 1.22 (30)
(range)	(−4.5 to 0)	(−4.0 to 1.25)
Axial length, mm (n)	23.3 ± 0.7 (23)	23.7 ± 0.8 (43)
Quadrants, n		
ST	24	26
SN	18	27
IT	16	35
IN	8	26

Data presented as mean ± standard deviation. Refractive error presented as spherical equivalent. N/A, not applicable.

Data Analysis

Average cone densities for each of the four retinal quadrants were compared between participants with and without diabetes using mixed model analysis. This method allows for unequal sample sizes of each retinal quadrant to be accounted for. To account for the nonindependence of retinal quadrants imaged within the same participant, an "id" variable was included as a random-effect term. The response variable, angular cone photoreceptor density, was analyzed. The fixed effects of the model included group (diabetes versus control), quadrant (superior temporal [ST], superior nasal [SN], inferior temporal [IT], inferior nasal [IN]), distance from the fovea, and group*quadrant interaction.

RESULTS

The demographic data for all participants are shown in the Table. There were no significant group differences in age, visual acuity, refractive error, or axial length. Most participants with T1D (18/29) were diagnosed before the age of 10. It is notable that HbA1c values in participants with T1D were significantly higher ($P < 0.01$) than recommended guidelines (<7%).

Sample Sizes

A total of 37 participants with diabetes (11 males, 26 females) and 61 control participants (19 males, 42 females) undertook AO retinal imaging. Usable images were extracted from 29 participants with diabetes (78%) and 44 control participants (72%). The most common causes for failure to extract usable images were excessive eye movements or failure of the AO system to focus correctly on the retina. Due to technical challenges, all four retinal quadrants were not imaged for every participant, and some data were discarded due to poor recording quality. The sample sizes for each quadrant imaged are included in the Table.

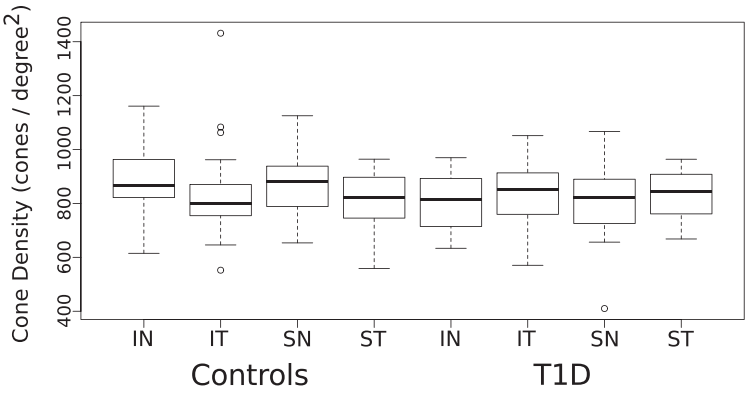

Figure 3. Distribution of cone density across the four retinal quadrants. *Boxes* represent the IQR; *whiskers* extend to all data points within 1.5 × IQR.

Axial Length

Axial length was measured in 23 participants with diabetes and 43 control participants. The remaining axial length measurements were missing because of unavailability of A-scan equipment. There was no significant difference in measured axial length between control participants and those with T1D.

Cone Density

Figure 3 compares angular cone densities between groups, in each retinal quadrant. There is no difference in cone photoreceptor density between groups (T1D mean = 821 ± 116 cones/deg^2; control mean = 849 ± 129 cones/deg^2; P = 0.46), or as cones/mm^2 (T1D mean = 10,298 ± 1635 cones/deg; control mean = 10,224 ± 1631 cones/deg; P = 0.60). Post hoc analysis reveals evidence for a radial asymmetry in control participants with reduced cone densities in the temporal retina compared with nasal retina (P = 0.01); this asymmetry was not observed in participants with T1D. There was no measurable influence of blood glucose control (HbA1c), duration of diabetes, or age on photoreceptor density.

Discussion

Cone photoreceptor density, in either angular or linear coordinates, was no different in the parafoveal retina of adolescents with T1D compared with control participants.

A recent study by Lombardo et al.[5] reported cone densities that were around 10% less in a population with T1D compared with controls. In the current study, we imaged more peripheral retinal regions (~2 mm peripheral versus a maximum of 460 μm). Our study population is younger (mean age in current study = 19 years versus 41 years) and is limited to participants with no DR. A factor perhaps of particular importance is the age at which participants were diagnosed with diabetes. In the current study, the age of diagnosis was 8.5 ± 4.1 years; the age of diagnosis in the study by Lombardo et al.[5] was 27 ± 8 years. This gives rise to the possibility that participants in the Lombardo et al.[5] study have undergone a prolonged period of undiagnosed diabetes with potentially poor control of insulin and glucose levels. Latent autoimmune diabetes in adults, an adult onset diabetes characterized by autoimmune attack on ß-cells and insulin resistance, should also be considered as an alternate diagnosis[20] for these older patients.

The cone densities observed in this study (25th–75th interquartile range [IQR], 8493–11,683 cones/mm^2) are in agreement with previously published data.[21,22] The observed nasal/temporal asymmetry in participants without T1D is consistent with that observed by Osterberg[23] and Curcio et al.[24] Interestingly, this asymmetry was not significant in the subjects with T1D (P = 0.26 for angular densities). The intersubject variability in cone densities are similar to those published by other groups working with both AO imaging and histologic data.[21,22]

The ability to observe cone photoreceptor structure reveals nothing about their function. Measures of retinal function such as the multifocal electroretinogram have revealed functional deficits in those with diabetes.[3,11,25] It is possible that deficits in photoreceptor function precede changes to photoreceptor structure and that the observed decrease in nasal/temporal asymmetry in our population with T1D may become more significant with increased disease duration.

A potential weakness of this study lies in the relatively small retinal regions selected for cone density analysis within each imaged area. While the region chosen for cone density analysis was placed without knowledge of the diabetic status of the participant, variations of cone density across the 1.8° imaged field may lead to a bias. An analysis of the position of the analyzed areas within each AOSLO image did not reveal any systematic differences between participants with diabetes and controls.

Difficulties obtaining images of suitable quality in all retinal areas of all subjects may introduce another source of variation. Retinal regions where it was not possible to image the cone mosaic were of necessity excluded from this study. A chi-squared test, comparing the imaging success rates of participants with T1D and control participants for each retinal quadrant, indicated no difference in success rates between the two groups. The reasons why imaging is not always possible are not clear but may be associated with reduced tear film breakup time associated with duration of T1D.[26]

In summary, this study demonstrates that cone photoreceptor density in the parafoveal retina of adolescents and young adults, with T1D, before the onset of retinopathy is similar to that of age similar control participants.

Acknowledgments

The authors thank retinal specialist Wai Ching Lam, MD, FRCSC, for grading fundus photographs; Marcia Wilson, RN, for monitoring the blood glucose levels of participants with diabetes during testing; Melissa Cotesta, OC(C), for conducting refractions; Aparna Bhan for coordinating clinical testing; and Cynthia VandenHoven, BAA, CRA, for fundus photography.

Supported by Canadian Institute for Health Research, Canadian Foundation for Innovation, and Natural Sciences and Engineering Research Council.

Disclosure: **W. Tan**, None; **T. Wright**, None; **D. Rajendran**, None; **Y. Garcia-Sanchez**, None; **L. Finkelberg**, None; **M. Kisilak**, None; **M. Campbell**, None; **C.A. Westall**, None

References

1. Bearse MA, Adams AJ, Han Y, et al. A multifocal electroretinogram model predicting the development of diabetic retinopathy. *Prog Retin Eye Res*. 2006;25:425–448.
2. Bresnick GH, Palta M. Oscillatory potential amplitudes: relation to severity of diabetic retinopathy. *Arch Ophthalmol*. 1987;105:929–933.
3. Lakhani E, Wright T, Abdolell M, Westall C. Multifocal ERG defects associated with insufficient long-term glycemic control in adolescents with type 1 diabetes. *Invest Ophthalmol Vis Sci*. 2010;51:5297–5303.
4. McFarlane M, Wright T, Stephens D, Nilsson J, Westall CA. Blue flash ERG PhNR changes associated with poor long-term glycemic control in adolescents with type 1 diabetes. *Invest Ophthalmol Vis Sci*. 2012;53:741–748.
5. Lombardo M, Parravano M, Lombardo G, et al. Adaptive optics imaging of parafoveal cones in type 1 diabetes. *Retina*. 2014; 34:546–557.
6. Park SH, Park JW, Park SJ, et al. Apoptotic death of photoreceptors in the streptozotocin-induced diabetic rat retina. *Diabetologia*. 2003;46:1260–1268.
7. Barber AJ, Lieth E, Khin SA, Antonetti DA, Buchanan AG, Gardner TW. Neural apoptosis in the retina during experimental and human diabetes: early onset and effect of insulin. *J Clin Invest*. 1998;102:783–791.
8. Tam J, Dhamdhere KP, Tiruveedhula P, et al. Disruption of the retinal parafoveal capillary network in type 2 diabetes before the onset of diabetic retinopathy. *Invest Ophthalmol Vis Sci*. 2011;52:9257–9266.
9. Burns SA, Elsner AE, Chui TY, et al. In vivo adaptive optics microvascular imaging in diabetic patients without clinically severe diabetic retinopathy. *Biomed Opt Express*. 2014;5:961–974.
10. Tan W, Wright T, Dupuis A, Lakhani E, Westall C. Localizing functional damage in the neural retina of adolescents and young adults with type 1 diabetes. *Invest Ophthalmol Vis Sci*. 2014;55:2432–2441.
11. Wright T, Cortese F, Nilsson J, Westall C. Analysis of multifocal electroretinograms from a population with type 1 diabetes using partial least squares reveals spatial and temporal distribution of changes to retinal function. *Doc Ophthalmol*. 2012;125:31–42.
12. Early Treatment Diabetic Retinopathy Study Research Group. Grading diabetic retinopathy from stereoscopic color fundus photographs–an extension of the modified Airlie House classification. ETDRS report number 10. *Ophthalmology*. 1991;98(suppl 5):786–806.
13. Hammer DX, Ferguson RD, Bigelow CE, et al. Adaptive optics scanning laser ophthalmoscope for stabilized retinal imaging. *Opt Express*. 2006;14:3354–3367.
14. Dubra A, Harvey Z. Registration of 2D images from fast scanning ophthalmic instruments. *Biomed Image Registr*. 2010;6204:60–71.
15. Coelho LP. Open source software for scriptable computer vision. *J Open Res Softw*. 2013;1:2013.
16. Lombardo M, Lombardo G, Ducoli P, Serrao S. Adaptive optics photoreceptor imaging. *Ophthalmology*. 2012;119:1498.
17. Otsu N. A threshold selection method from gray-level histograms. *IEEE Trans Syst Man Cybern*. 1979;9:62–66.
18. Chiu SJ, Lokhnygina Y, Dubis AM, et al. Automatic cone photoreceptor segmentation using graph theory and dynamic programming. *Biomed Opt Express*. 2013;4:924–937.
19. Garrioch R, Langlo C, Dubis AM, Cooper RF, Dubra A, Carroll J. Repeatability of in vivo parafoveal cone density and spacing measurements. *Opt Vis Sci*. 2012;89:632–643.
20. Redondo MJ. LADA: time for a new definition. *Diabetes*. 2013; 62:339–340.
21. Curcio CA, Sloan KR, Kalina RE, Hendrickson AE. Human photoreceptor topography. *J Comp Neurol*. 1990;292:497–523.
22. Chui TY, Song H, Burns SA. Adaptive-optics imaging of human cone photoreceptor distribution. *J Opt Soc Am A Opt Image Sci Vis*. 2008;25:3021–3029.
23. Osterberg GA. Topography of the layer of rods and cones in the human retina. *Acta Ophthalmol*. 1935;13:11–103.
24. Curcio C, Sloan K, Packer O. Distribution of cones in human and monkey retina: individual variability and radial asymmetry. *Science*. 1987;579–582.
25. Han Y, Bearse MA, Schneck ME, Barez S, Jacobsen CH, Adams AJ. Multifocal electroretinogram delays predict sites of subsequent diabetic retinopathy. *Invest Ophthalmol Vis Sci*. 2004;45:948–954.
26. Akinci A, Cetinkaya E, Aycan Z. Dry eye syndrome in diabetic children. *Eur J Ophthalmol*. 2007;17:873–878.

Investigative Ophthalmology & Visual Science